DISTRIBUTED VOLUME RENDERING FOR SCALABLE HIGH-RESOLUTION DISPLAY ARRAYS

Nicholas Schwarz
Northwestern University, U.S.A.

Jason Leigh
Electronic Visualization Laboratory (EVL), University of Illinois at Chicago (UIC), U.S.A.

Keywords: High-resolution display arrays, Direct volume rendering, Parallel rendering, Graphics systems and distributed shared-memory.

Abstract: This work presents a distributed image-order volume rendering approach for scalable high-resolution displays. This approach preprocesses data into a conventional hierarchical structure which is distributed across the local storage of a distributed-memory cluster. The cluster is equipped with graphics cards capable of hardware accelerated texture rendering. The novel contribution of this work is its unique data management scheme that spans both GPU and CPU memory using a multi-level cache and distributed shared-memory system. Performance results show that the system scales as output resolution and cluster size increase. An implementation of this approach allows scientists to quasi-interactively visualize large volume datasets on scalable high-resolution display arrays.

1 INTRODUCTION

The spatial resolution of data collected by scientific instruments is increasing. Thus, the volume data with which scientists work is increasing in size. For example, bio-scientists use multi-photon microscopes to image fluorescent structures deep in tissue at unprecedented resolutions. Smaller image sections collected from in situ or in vivo experiments group together to form large image montages. Layers of montages are stacked to form large volumes. Although these volumes are shallow, useful insight may be gained with free-form navigation and off-axis projections.

Currently, scientists visualize such large datasets on desktop displays that typically have only a few million pixels. These displays constrain the way in which scientists analyze spatially large volume data. Scientists view either a low-resolution image that represents the entire spatial extent of the data but neglects detail, or small portions of the data in high-resolution but loose spatial context.

Our experience shows that high-resolution displays allow scientists to see their spatially large data at or nearer its native resolution, and are experiencing an increasing rate of adoption within the scientific community. Most often, scalable high-resolution displays are composed of an array of liquid-crystal displays (LCDs) or projectors and a commodity distributed-memory cluster of computers with accelerated graphics hardware.

Scientists require a direct volume visualization solution for commodity-off-the-shelf (COTS) distributed-memory clusters that scales with respect to large input data, i.e. data too large to conveniently replicate across all processors, and produces high-resolution output for high-resolution displays. However, most parallel volume rendering research concentrates on rendering large data at output resolutions that are small in comparison to the resolution provided by a high-resolution display array. As shown in the next section, parallel volume rendering research that specifically focuses on producing high-resolution output employs data replication, or requires the use of specialized hardware.

This work presents a distributed image-order volume rendering approach for scalable high-resolution displays. It uses a unique multi-level cache and distributed shared-memory system that

Schwarz N. and Leigh J. (2010).
DISTRIBUTED VOLUME RENDERING FOR SCALABLE HIGH-RESOLUTION DISPLAY ARRAYS.
In *Proceedings of the International Conference on Computer Graphics Theory and Applications*, pages 211-218
DOI: 10.5220/0002812902110218

Table 1: Overview of direct volume rendering work in terms of output resolution and input data size. †Although this architecture may potentially scale to support high-resolution display arrays, neither a theoretical nor a practical implementation have shown the system's ability to scale in terms of output resolution.

Data Size	Output Resolution	
	Low	High
Small	(Cabral et al., 1994) (Grzeszczuk et al., 1998) (Ikits et al., 2004) (Kruger and Westermann, 2003) (Lacroute and Levoy, 1994) (Levoy, 1988) (Pfister et al., 1999) (Rezk-Salama et al., 2000) (Westover, 1990)	(McCorquodale and Lombeyda, 2003) (Schwarz et al., 2004)
Large	(Bajaj et al., 2000) (Camahort and Chakravarty, 1993) (Elvins, 1992) (Hsu, 1993) (Ino et al., 2003) (Lombeyda et al., 2001) (Palmer et al., 1998) (Peterka et al., 2008) (Ma et al., 1994) (Marchesin et al., 2008) (Mller et al., 2006) (Muraki et al., 2003)	(Lombeyda et al., 2001)†

spans both GPU and CPU memory, along with a conventional preprocessed hierarchical data structure and hardware accelerated rendering to visualize large input data on output displays connected to distributed-memory clusters. Scientists successfully use an implementation of this approach, Vol-a-Tile 2, to visualize two large microscopy datasets, described later, on two LCD arrays.

2 BACKGROUND

Volume renderers evaluate a common optical model. A number of serial techniques have been developed to accomplish this task that operate in software (Levoy, 1988; Westover, 1990; Lacroute and Levoy, 1994), rely on hardware with texture mapping capabilities (Cabral et al., 1994; Grzeszczuk et al., 1998; Rezk-Salama et al., 2000), or use advanced graphics-processing unit (GPU) methods (Kruger and Westermann, 2003; Ikits et al., 2004). Additionally, special purpose hardware, such as the VolumePro graphics card (Pfister et al., 1999), have been designed specifically for volume rendering.

Parallel techniques have been developed to increase performance and render larger datasets. The optimal choice of parallelization technique and rendering method is heavily dependent on the implementation architecture.

Parallel image-order techniques, also referred to as sort-first techniques, break the output image into disjoint regions and assign a processing unit to render everything in that region. Image-order implementations have been developed for shared-memory systems (Palmer et al., 1998) as well as distributed-memory systems (Bajaj et al., 2000).

Parallel object-order methods, also referred to as sort-last methods, assign a processing unit to a section of data regardless of where the data appears in the final output image. After each section of data is rendered, a compositing step based on the theory described by Porter and Duff (1984) constructs the final image. Much effort has been devoted to developing efficient compositing methods (Hsu, 1993; Camahort and Chakravarty, 1993; Ma et al., 1994; Ino et al., 2003). Object-order implementations have been developed for distributed-memory clusters (Elvins, 1992; Mller et al., 2006; Marchesin et al., 2008) and modern supercomputers (Peterka et al., 2008), and specialized hardware has been developed that implements the binary-swap compositing method (Lombeyda et al., 2001; Muraki et al., 2003).

Table 1 gives an overview of direct volume rendering work in terms of output resolution and data size. The left column shows some of the large body of direct volume rendering work that renders low output resolution images. The right column shows that very little research exists specifically addressing the production of output for high-resolution display arrays.

According to Lombeyda et al. (2001), the Sepia-2 hardware compositing architecture may potentially scale to support high-resolution display arrays. The Sepia-2 system uses a sort-last compositing approach to assemble image portions produced by VolumePro graphics cards on a distributed-memory cluster. However, contrary to the name of the paper in which it was published, this system uses proprietary hardware components that are no longer available. In addition, neither a theoretical nor a practical implementation

Table 2: Comparison of parallel high-resolution volume rendering systems with regard to large data, high-resoltuion output and operating on commodity-off-the-shelf (COTS) distributed-memory clusters. †Neither a theoretical nor a practical implementation have shown this system's ability to scale in terms of output resolution, although the publication claims it may potentially scale to support high-resolution display arrays.

System	Attribute		
	Large Data	High-Resolution	COTS
Sepia-2 (Lombeyda et al., 2001)	✓	✓†	✗
Volume Visualizer (McCorquodale and Lombeyda, 2003)	✗	✓	✓
Vol-a-Tile (Schwarz et al., 2004)	✗	✓	✓
Vol-a-Tile 2	✓	✓	✓

has shown the system's potential to scale in terms of output resolution.

The TeraVoxel project produced Volume Visualizer (McCorquodale and Lombeyda, 2003), a solution for high-resolution displays. Using a cluster equipped with four VolumePro cards, the system is able to render a 256 x 256 x 1,024 volume to the 3,840 x 2,400 output window of a ten mega-pixel IBM T221 LCD. This is accomplished by replicating the entire dataset on all four nodes of the cluster.

Vol-a-Tile (Schwarz et al., 2004) is a direct volume rendering application designed for scalable high-resolution displays. Users roam through large volume datasets that may be stored remotely, viewing small regions-of-interest in full resolution. The data within a region-of-interest is replicated on the graphics card in every node where it is culled based on view and rendered using 3D texture-mapping. When the region changes, each node uploads identical copies of the new data for the region.

Table 2 compares this work to current volume rendering systems for high-resolution displays. This work expands the capabilities of current systems by providing a direct volume rendering solution for high-resolution displays that operates on COTS distributed-memory clusters and does not require data replication.

3 METHODOLOGY

This system uses the parallel image-order data decomposition approach illustrated in Figure 1. First, data is preprocessed into a hierarchical data structure and the view-frustum for each node is computed. When the system is running, the user interactively determines the view-transformation via a separate user-interface. For each node, a list of visible bricks is created and sorted. The rendering component renders each brick, swapping buffers when it reaches the end of each level-of-detail. The output image is displayed in place on the node that rendered it. The data management system uses a distributed shared-memory system and a multi-level cache to distribute and relocate data on the cluster according to the view-transformation.

3.1 Hierarchical Data Structure

This system uses a conventional octree data structure to represent volume data. Octrees are not new (Knoll, 2006). They are used because they provide the ability to progressively render data, allowing for faster interaction. Each level of the tree is associated with a different level-of-detail representation of the original data. The leaf nodes are associated with the original, highest resolution data. The root node is associated with the coarsest resolution data. Octree based representations have been used successfully to manage large datasets (LaMar et al., 1999; Weiler et al., 2000; Plate et al., 2002).

In the event that one of the dimensions of the data is substantially smaller than the others, an octree may not be appropriate. In this case, four leaf nodes are left empty, producing a quadtree-like data structure. Data along the short dimension is not subsampled at each level like in the octree. Besides this, all other algorithms function on both data structures without modification.

3.2 Data Management

The data management system is critical to the system's ability to render large data on a distributed-memory cluster. This approach uses a memory system similar to distributed shared-memory architectures. It keeps track of data bricks loaded in RAM across all nodes of the cluster, and transfers bricks between nodes when required.

A multi-level cache system keeps the most recently used data bricks as close to the graphics hardware as possible. The first level of the cache resides in the texture-memory of each graphics card. The second level exists in the main memory of each

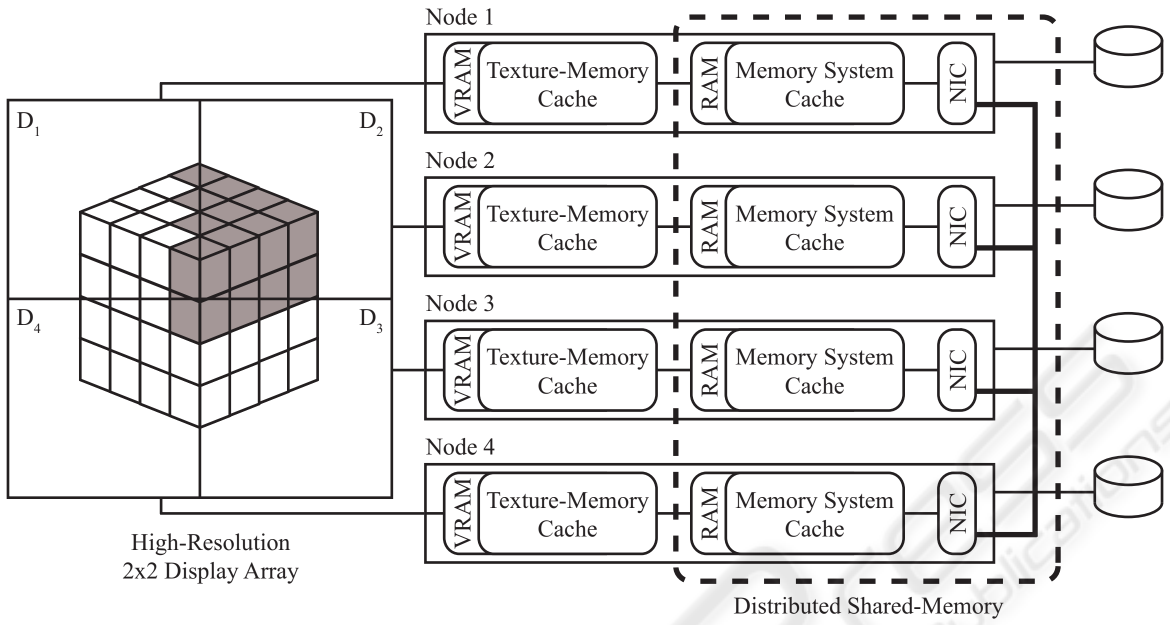

Figure 1: Parallel image-order volume rendering approach for a high-resolution display array. Bricks are rendered by the nodes on which they appear. In this case, the leaf nodes of an octree three levels deep are shown on a 2x2 display array and a four node cluster connected via a high-speed backplane. The shaded bricks are those rendered on Node 2. The data management system, comprising of a two-level cache and a distributed shared-memory system, is responsible for rearranging bricks on the cluster based on the view-transformation.

node. Both cache levels employ the least-recently-used (LRU) replacement strategy. The number of bricks in each cache is determined by the allotted memory, set by the user, divided by the brick size.

The texture-memory cache keeps as many of the most recently used data bricks as possible resident in texture-memory. When the rendering component requests a particular brick, the texture-memory cache is the first place the data management system searches. If the brick is found, it is moved to the top of the cache and its texture data is reported to the renderer. If the brick is not present, the data management system continues its search at the next level until it finds the brick and inserts it at the top of the texture-memory cache. This process may push LRU bricks out of the texture-memory cache.

The second cache level is the memory system cache. This cache keeps as many of the most recently used bricks requested by an individual node in the local RAM of the requesting node as possible. The data management system searches this cache when a brick is not found in the texture-memory cache.

When the memory system cache receives a request for a brick, it checks the bricks currently in the cache. If the brick is present, it is moved to the top of the cache and the data management system inserts the brick in the texture-memory cache. If it is not present, a query is made to the distributed shared-memory system. Once the brick is retrieved, it is placed at the top of the cache. This cache, like the texture-memory cache, may push LRU bricks out.

The distributed shared-memory system keeps track of all bricks loaded in each node's memory system cache. The system can query a brick using the brick's ID value stored along with the volume's tree metadata. If a node requires a brick present on another node, the distributed shared-memory system transfers it to the recipient node via the cluster's high-speed backplane. In the event that a brick is not present in any memory system cache, the data management system loads the data from the local disk on which it resides, transfers it to the recipient node via the same mechanism as the distributed shared-memory system uses, and loads it in the recipient node's cache.

Prior to running the system, the preprocessed bricks are distributed in a round-robin, level-by-level fashion among cluster nodes, where they are stored on local disks. If there are too few bricks in a level to place at least one brick on each node, the entire level is replicated on every node. This replication is feasible because typically only the first few levels are replicated requiring very little overhead.

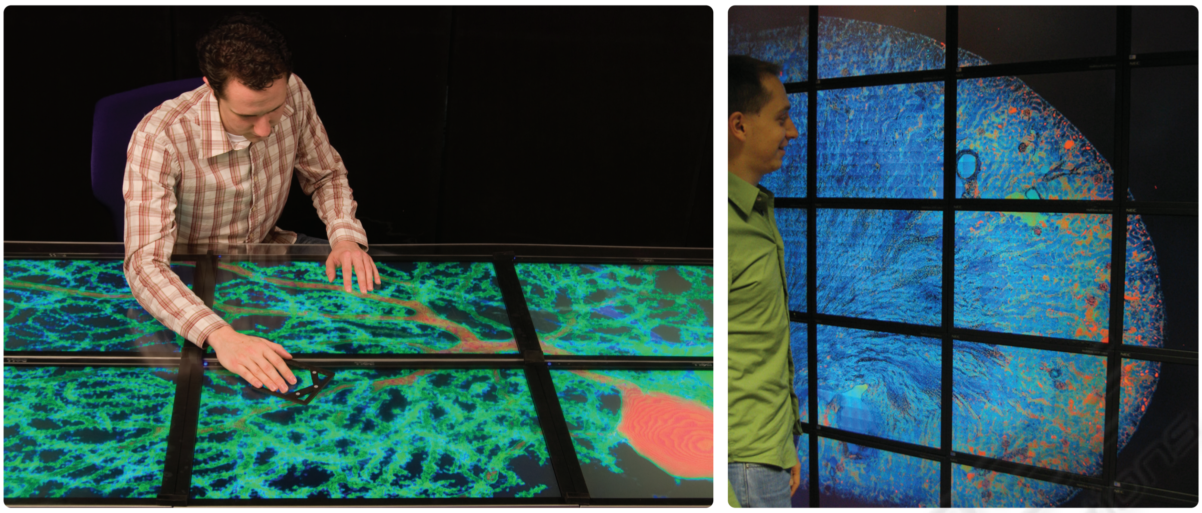

(a) Purkinje Neuron (b) Rat Kidney

Figure 2: Example datasets rendered on two high-resoution display arrays. (a) Researcher exploring the Purkinje neuron dataset on a twenty-four megapixel tabletop display. (b) Scientist examining the rat kidney dataset on a 100 megapixel display.

Table 3: Test properties and performance evaluation results for the Visible Human Female CT, Purkinje neuron, and rat kidney datasets. The original dimensions and sizes are given for each dataset along with the brick dimensions, brick size, and total size of each preprocessed tree. The rightmost column shows the speed-up factor relative to the lowest performing brick size.

Data	Original Dimensions	Original Size	Brick Dimensions	Brick Size	New Size	Speed-up
Human	512 x 512 x 2048 16-bit	1 GB	64 x 64 x 256	2 MB	1.14 GB	2.3
			32 x 32 x 128	256 KB		1.0
Purkinje	2048 x 4096 x 128 16-bit	2 GB	128 x 256 x 128	8 MB	2.66 GB	1.0
			64 x 128 x 128	2 MB		2.2
			32 x 64 x 128	512 KB		1.9
Kidney	32,768 x 32,768 x 128 24-bit	384 GB	256 x 256 x 128	8 MB	512 GB	1.0
			128 x 128 x 128	6 MB		2.1
			64 x 64 x 128	1.5 MB		2.4
			32 x 32 x 128	384 KB		1.9

3.3 Rendering and Interaction

Based on its frustum and the current view transformation, each node independently creates a list of visible bricks using a breadth-first search algorithm to traverse the octree. Each node then uses hardware accelerated 3D texture-mapping (Kniss et al., 2001; Ikits et al., 2004) to render its visible list of bricks. Each brick is rendered as its own individual texture. The data management system ensures the necessary textures are loaded in texture-memory. In the case where data bricks cross tile boundaries, the bricks are copied to each node where they are visible.

The opacity assigned at each sample point must be corrected to account for the number of samples taken and the current octree level. This situation occurs when the user changes the sampling rate via the user-interface, and when the renderer switches to a different level-of-detail. This is especially important when viewing a large, shallow volume from the side, as the number of slices is much greater than when viewed from the top.

The level-of-detail mechanism automatically switches to using the coarsest resolution data whenever the user interacts. This allows the user instant feedback based on navigation without waiting for a dataset to be fully rendered. When the user stops navigation, the system progressively renders higher resolution data from successive levels of the octree giving the user an image of continuously increasing detail.

4 RESULTS

The system was tested on two microscopy datasets: a Purkinje neuron sampled from a rat brain and a rat kidney. For comparison to a widely known dataset, the Visible Human Female CT dataset was evaluated. Each dataset was tested with trees of varying levels and brick sizes to determine which brick size, and thus tree depth, produced the best results. The number of voxels along each dimension of a brick is a power of two in order to meet the texture requirements of the graphics cards. Brick sizes were increased until they exceeded the texture-size limitation of the graphics hardware. The rendering time was measured at increasing output resolutions for each dataset using the best performing brick size for each respective dataset. The number of rendering nodes was increased along with output resolution to suit the testbed's hardware constraints.

The Purkinje dataset in Figure 2(a) is shown on a six panel, twenty-four megapixel tabletop display. The original raw data creates a 2,048 x 4,096 x 128 volume of 16-bit voxels. The real spatial extent of the data is about $80\,\mu m$ x $80\,\mu m$ x $15\,\mu m$. The display is run by a three node cluster where each node is attached to two 2,560 x 1,600 LCDs. Each cluster node has one AMD Athlon 64 FX-60 Dual Core processor, 2 GB of RAM, and a PCI-E nVidia GeForce 7900 GT graphics card with 256 MB of texture-memory. The cluster is connected via a 10 Gbps Ethernet backplane with the MTU size set to 9,000 bytes.

The rat kidney dataset in Figure 2(b) is shown on a fifty-five panel, 100 megapixel display. The original raw data comprises a 32,768 x 32,768 x 128 volume of 24-bit samples. The real spatial extent of the data is about $8\,mm$ x $5\,mm$ x $1.5\,mm$. The display is run by a twenty-eight node cluster where all but one node is attached to two 1,600 x 1,200 LCDs. Each cluster node has two AMD Opteron 246 processors, 4 GB of RAM, 500 GB of local storage space, and an 8x AGP nVidia Quadro FX 3000 graphics card with 256 MB of texture-memory. The cluster is connected via a 1 Gbps Ethernet backplane with the MTU size set to 9,000 bytes.

The Visible Human Female CT dataset was tested on the same tabletop display as the Purkinje neuron dataset. The original 512 x 512 x 1,871 volume was padded to form a 512 x 512 x 2,048 volume, and the voxel resolution was increased from 12-bits to 16-bits. This was done to satisfy the volume renderer's texture size requirements.

The system is written in C++ using the OpenGL, Cg and MPICH libraries. All test computers are running the openSUSE 10.2 Linux distribution.

Table 3 shows the average speed-up factor for each brick size of the Visible Human Female CT and Purkinje neuron datasets rendered at twenty-four megapixels on three nodes. Table 3 also shows the average speed-up factor for each of the rat kidney dataset's brick sizes when rendered at 100 megapixels on twenty-eight nodes. The Visible Human Female CT dataset performed best with a brick size of 64 x 64 x 256. The Purkinje neuron dataset performed best when using a brick size of 64 x 128 x 128. The rat kidney rendered fastest using a brick size of 64 x 64 x 128.

Preprocessing datasets into an octree or quadtree increases the size of each dataset as new data is generated for each level-of-detail. This process is performed once for each dataset using an offline tool, and stored for later use. The Visible Human dataset was converted into an octree, while the Purkinje neuron and rat kidney datasets were converted into the quadtree-like structure described earlier due to their relative flatness. The original dataset sizes as well as the new sizes after preprocessing are shown in Table 3. Because the data collection process is not coupled with visualization and may take on the order of days to weeks to complete, the additional time to preprocess data is acceptable.

Table 4 shows the average time to render a single frame of the Visible Human Female CT, Purkinje neuron and rat kidney datasets. These results reflect the average time taken to render and display all data in all levels of the tree at various rotations. The results show that as the output resolution increases along with the corresponding number of rendering nodes, the time taken to render each dataset decreases. Total rendering time is also reduced when zooming in due to culling data from the scene.

When the user changes the viewing parameters the system switches to the lowest level-of-detail giving the user a quasi-interactive experience. The lowest level-of-detail is always the size of one brick. In all test cases the lowest level-of-detail renders at interactive rates.

5 CONCLUSIONS

A distributed image-order volume rendering system for scalable high-resolution display arrays was presented. The successful image-order decomposition of data was made possible by using a specialized data management system that manages data across both GPU and CPU memory. Results were presented showing the system's performance

Table 4: Performance results for test datasets as output resolution and cluster size increases using the best performing brick size for each dataset.

Data	Megapixels	Nodes	Time/Frame (seconds)
Human	8	1	2.1
	16	2	0.6
	24	3	0.3
Purkinje	8	1	3.4
	16	2	1.7
	24	3	0.5
Kidney	15	4	2625
	30	8	1100
	60	16	525
	92	25	230
	100	28	198

using different brick sizes on real datasets. The results show that the system scales as output resolution and cluster size increase. The increase in performance observed as the output resolution increases is due to the reduction in the number of bricks each node must render as the cluster size also increases. An increase in the number of rendering nodes reduces the number of texture lookups along the viewing direction, the amount of texture uploads to the GPU, the amount data transfer among nodes and the number of disk accesses. In the future we hope to better evaluate the system's performance and suggest areas for improvement by analyzing cache misses and rendering, network and I/O bottlenecks.

ACKNOWLEDGEMENTS

Biological datasets and insight graciously provided by Rajvikram Singh, Thomas Deerinck, Hiroyuki Hakozaki, Diana Price, Masako Terada and Mark Ellisman of the National Center for Microscopy and Imaging Research (NCMIR) at the University of California, San Diego (UCSD).

Special thanks to Lance Long, Patrick Hallihan and Alan Verlo for their expert advice and support.

Work at Northwestern University is supported in part by Children's Memorial Research Center, Children's Memorial Hospital, and from the National Institute of Neurological Disorders and Stroke (NINDS) grant 1 P30 NS054850-01A1.

The Electronic Visualization Laboratory (EVL) at the University of Illinois at Chicago (UIC) specializes in the design and development of high-resoltuion visualization and virtual-reality display systems, collaboration software for use on multi-gigbit networks, and advanced networking infrastructure. Work at EVL is supported by the National Science Foundation (NSF), awards CNS-0420477, CNS-0703916, OCI-0441094 and OCE-0602117, as well as the NSF Information Technology Research (ITR) cooperative agreement (OCI-0225642) to the University of California, San Diego (UCSD) for "The OptIPuter". EVL is also supported by funding from the National Institutes of Health, the State of Illinois, the Office of Naval Research on behalf of the Technology Research, Education, and Commercialization Center (TRECC), and Pacific Interface on behalf of NTT Optical Network Systems.

REFERENCES

Bajaj, C., Ihm, I., Park, S., and Song, D. (2000). Compression-based ray casting of very large volume data in distributed environments. In *HPC '00: Proceedings of the The Fourth International Conference on High-Performance Computing in the Asia-Pacific Region-Volume 2*, pages 720–725.

Cabral, B., Cam, N., and Foran, J. (1994). Accelerated volume rendering and tomographic reconstruction using texture mapping hardware. In *VVS '94: Proceedings of the 1994 symposium on Volume visualization*, pages 91–98.

Camahort, E. and Chakravarty, I. (1993). Integrating volume data analysis and rendering on distributed memory architectures. In *PRS '93: Proceedings of the 1993 symposium on Parallel rendering*, pages 89–96.

Elvins, T. T. (1992). Volume rendering on a distributed memory parallel computer. In *VIS '92: Proceedings of the 3rd conference on Visualization '92*, pages 93–98.

Grzeszczuk, R., Henn, C., and Yagel, R. (1998). Advanced geometric techniques for ray casting volumes. In *SIGGRAPH '98: ACM SIGGRAPH 1998 courses*.

Hsu, W. M. (1993). Segmented ray casting for data parallel volume rendering. In *PRS '93: Proceedings of the 1993 symposium on Parallel rendering*, pages 7–14.

Ikits, M., Kniss, J., Lefohn, A., and Hansen, C. (2004). *GPU Gems*, chapter 39, pages 667–691. Addison Welsey.

Ino, F., Sasaki, T., Takeuchi, A., and Hagihara, K. (2003). A divided-screenwise hierarchical compositing for sort-last parallel volume rendering. In *IPDPS '03: Proceedings of the 17th International Symposium on Parallel and Distributed Processing*, page 14.1.

Kniss, J., McCormick, P., McPherson, A., Ahrens, J., Painter, J., Keahey, A., and Hansen, C. (2001). Interactive texture-based volume rendering for large datasets. *IEEE Computer Graphics & Applications*, 21(4):52–61.

Knoll, A. (2006). A survey of octree volume rendering techniques. In *Visualization of Large and Unstructured Data Sets*, pages 87–96.

Kruger, J. and Westermann, R. (2003). Acceleration techniques for gpu-based volume rendering. In *VIS '03: Proceedings of the 14th IEEE Visualization 2003 (VIS'03)*, pages 287–292.

Lacroute, P. and Levoy, M. (1994). Fast volume rendering using a shear-warp factorization of the viewing transformation. In *SIGGRAPH '94: Proceedings of the 21st annual conference on Computer graphics and interactive techniques*, pages 451–458.

LaMar, E., Hamann, B., and Joy, K. I. (1999). Multiresolution techniques for interactive texture-based volume visualization. In *VIS '99: Proceedings of the conference on Visualization '99*, pages 355–361.

Levoy, M. (1988). Display of surfaces from volume data. *IEEE Computer Graphics and Applications*, 8(3):29–37.

Lombeyda, S., Moll, L., Shand, M., Breen, D., and Heirich, A. (2001). Scalable interactive volume rendering using off-the-shelf components. In *PVG '01: Proceedings of the IEEE 2001 symposium on parallel and large-data visualization and graphics*, pages 115–121.

Ma, K.-L., Painter, J. S., Hansen, C. D., and Krogh, M. F. (1994). Parallel volume rendering using binary-swap compositing. *IEEE Comput. Graph. Appl.*, 14(4):59–68.

Marchesin, S., Mongenet, C., and Dischler, J.-M. (2008). Multi-gpu sort-last volume visualization. In *Eurographics Symposium on Parallel Graphics and Visualization (EGPGV08)*.

McCorquodale, J. and Lombeyda, S. V. (2003). The volumepro volume rendering cluster: A vital component of parallel end-to-end solution. Technical report, California Institute of Technology.

Muraki, S., Lum, E. B., Ma, K.-L., Ogata, M., and Liu, X. (2003). A pc cluster system for simultaneous interactive volumetric modeling and visualization. In *PVG '03: Proceedings of the 2003 IEEE Symposium on Parallel and Large-Data Visualization and Graphics*, pages 95–102.

Mller, C., Strengert, M., and Ertl, T. (2006). Optimized volume raycasting for graphics-hardware-based cluster systems. In *Eurographics Symposium on Parallel Graphics and Visualization (EGPGV06)*, pages 59–66.

Palmer, M. E., Totty, B., and Taylor, S. (1998). Ray casting on shared-memory architectures: Memory-hierarchy considerations in volume rendering. *IEEE Concurrency*, 6(1):20–35.

Peterka, T., Yu, H., Ross, R., and Ma, K.-L. (2008). Parallel volume rendering on the ibm blue gene/p. In *Eurographics Symposium on Parallel Graphics and Visualization (EGPGV08)*.

Pfister, H., Hardenbergh, J., Knittel, J., Lauer, H., and Seiler, L. (1999). The volumepro real-time ray-casting system. In *SIGGRAPH '99: Proceedings of the 26th annual conference on Computer graphics and interactive techniques*, pages 251–260.

Plate, J., Tirtasana, M., Carmona, R., and Fröhlich, B. (2002). Octreemizer: a hierarchical approach for interactive roaming through very large volumes. In *VISSYM '02: Proceedings of the symposium on Data Visualisation 2002*, pages 53–60.

Porter, T. and Duff, T. (1984). Compositing digital images. In *SIGGRAPH '84: Proceedings of the 11th annual conference on Computer graphics and interactive techniques*, pages 253–259.

Rezk-Salama, C., Engel, K., Bauer, M., Greiner, G., and Ertl, T. (2000). Interactive volume rendering on standard pc graphics hardware using multi-textures and multi-stage rasterization. In *HWWS '00: Proceedings of the ACM SIGGRAPH/EUROGRAPHICS workshop on Graphics hardware*, pages 109–118.

Schwarz, N., Venkataraman, S., Renambot, L., Krishnaprasad, N., Vishwanath, V., Leigh, J., Johnson, A., Kent, G., and Nayak, A. (2004). Vol-a-tile - a tool for interactive exploration of large volumetric data on scalable tiled displays. In *VIS '04: Proceedings of the conference on Visualization '04*, page 598.19.

Weiler, M., Westermann, R., Hansen, C., Zimmermann, K., and Ertl, T. (2000). Level-of-detail volume rendering via 3d textures. In *VVS '00: Proceedings of the 2000 IEEE symposium on Volume visualization*, pages 7–13.

Westover, L. (1990). Footprint evaluation for volume rendering. In *SIGGRAPH '90: Proceedings of the 17th annual conference on Computer graphics and interactive techniques*, pages 367–376.